Proceedings of the 10^{th} Brazilian Congress of Thermal Sciences and Engineering – ENCIT 2004
Braz. Soc. of Mechanical Sciences and Engineering – ABCM, Rio de Janeiro, Brazil, Nov. 29 – Dec. 03, 2004

Paper CIT04-0046

EXPERIMENTAL ANALYSIS OF THE INFLUENCE OF PULSATION FREQUENCY ON THE TURBULENCE OF PULSATILE FLOWS

de Paula, Igor Braga
Escola de Engenharia de São Carlos – Depto Eng. de Materiais, Aeronáutica e Automobilística
Av. Trabalhador Sancarlense n°400, CEP 13566-590 – São Carlos, SP, Brasil
igorbrag@terra.com.br

de Medeiros, Marcello A. Faraco
Escola de Engenharia de São Carlos – Depto Eng. de Materiais, Aeronáutica e Automobilística
Av. Trabalhador Sancarlense n°400, CEP 13560-270 – São Carlos, SP, Brasil
marcello@sc.usp.br

Abstract. *This work presents the results of an experimental study of pulsatile flows in pipes. A pulsatile flow is characterized by the presence of velocity fluctuations of low frequencies and large amplitudes. This type of flow can be found in many practical applications, such as internal combustion engines and biological flows. The parameters considered in this study were the Reynolds number and the pulsation frequency. The method used for analysing the data showed the variation of the turbulence intensity along the pulsation cycle. It was found that the peak of turbulence intensity does not coincide with the peak of the pulsating base flow. The phase shift was calculated using cross correlation techniques. In the parameter range tested the relationship between the phase shift and the frequency of pulsation was well correlated by linear regression. Velocity measurements were made with a constant temperature hot wire anemometer.*

keywords: *pulsating flows, turbulence, hot-wire anemometry*

1. Introduction

Time-periodic flows can be classified in two different categories: pulsatile flows and oscillatory flows. In the pulsatile type there is only one flow direction and the mean velocity is different from zero, whereas in oscillatory flows the mean velocity is zero and the presence of reverse flow is always observed. Time-periodic flows can be either laminar, transitional or turbulent. According to Fishler and Brodkey, 1991 the flow regime can change along the pulsation period. Turbulent pulsatile flows show clearly the presence of two kinds of velocity fluctuation, one of low frequency and another of high frequency. Separating the flow into a mean and a turbulent part, the velocity can be written as:

$$U(t) = \overline{U}(t) + u'(t) \tag{1}$$

where $U(t)$ is the total velocity, $\overline{U}(t)$ is the mean flow, which is composed by the mean velocity and the low frequency fluctuation, and $u'(t)$ is the turbulent component. Note that in this flow we consider a time variation of the mean velocity.

A pulsatile flow can be experimentally studied using ensemble average techniques, but it is necessary a good control of flow parameters such as frequency and amplitude of pulsation. However some techniques have been developed to minimize the need of such sofisticated control. Catania and Mitica, 1989 show a review about some of this techniques in their study about turbulent flows in cylinders of internal combustion engines. According to Catania and Mitica, 1992 the most powerful technique is the spectral filtering. This technique was applied in the current study.

2. Experimental Facility

A experimental facility was designed and built to run experiments. A scheme of the apparatus is shown in figure 1. The arrangement used a single fan connected to a PVC tube with 45mm in diameter and 5000mm in length. This ensured that the flow was fully developed at the measuring station. The Reynolds number of the flow was limited by the power of the fan. A manual valve was placed next to the fan to set the flow velocity. This type of valve cannot provide a good control of the flow parameters. It was used because of its simple operation and low cost. Downstream it was placed a fine stainless-steel wire screen. This provided a more uniform flow and reduced the scale of turbulence structures.

During the experiments the velocity was measured using a hot wire anemometer. A static pitot tube connected to an inclined manometer with a estimated precision of 2.0Pa were used in the calibration of the anemometer. During the experiments the temperature variation was monitored with a type K termopar. The output voltage of the anemometer was filtered by an anti-aliasing filter before digital acquisition . The data was collected in a 16-bits resolution channel in a

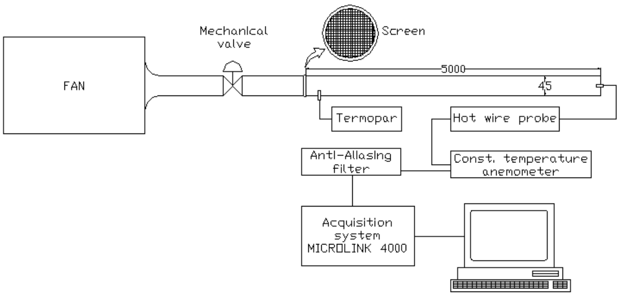

Figure 1: Experimental arrangement

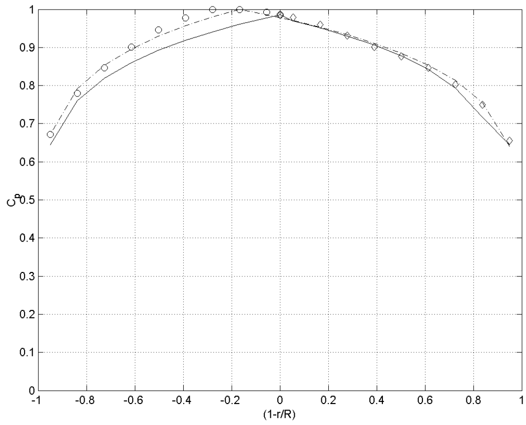

Figure 2: Velocity profile - $\diamondsuit$ measured values, . . . power law with u_c and R at the center,$- \cdot -$ power law with u_c and R at the maximum velocity

512Kb buffer. The sample frequency was set to 10kHz with an acquisition period of 1 second. As suggested by Möller, 2000 the anti-aliasing filter was set to 1/3 of the sample frequency.

3. Experimental Procedure

Before studying the effect of the pulsation on the flow in the pipe, the steady case was measured. The velocity profile measured is shown by $\diamondsuit$ in the figure 2. The distance between each measurement point was 2.5mm. Close to the pipe wall the distance was not 0 because of the radius of the pitot tube.

The velocity profile was compared with the power law described in Schlichting, 1979:

$$\frac{u_m}{u_c} = \left(1 - \frac{r}{R}\right)^{\frac{1}{n}} \tag{2}$$

where u_m is the flow velocity at each point measured, u_c is the velocity at the center of the pipe, r is the instant radial position, R is the tube radius and N is the power exponent. The value n was chosen to be 7. The power law for this case is shown in fig. 2 by the dotted line. Only the profile showed in the right side of the figure 2 was well correlated with the theoretical values. Observing the figure we can infer that the velocity profile is slightly asymmetrical. We attempt to reduce this effect by the rotation of the tube after each set of measurements, but it did not work. However, the asymmetry was considered sufficient for the current purpose. To achieve a better agreement between the theoretical profile and the measured profile we assumed u_c and R as the maximum velocity and the maximum velocity point respectively, instead of the center values. The dashed line in the figure 2 shows the power law behavior for this case. It seems to be well correlated with the profile measured at both sides of the tube.

The results showed that the center part of the pipe had a reasonable flat profile. This region was used to place the static pitot and the hot wire probe in the calibration procedure of the hot wire anemometer. The calibration data was fit to a King's law [Perry, 1982] written in the form:

$$E^2 = A + BU^n \tag{3}$$

where E is the output voltage of the anemometer, U is the velocity measured using the static-pitot, A, B and n are coefficients to be adjusted in calibration procedure. In general the value for n range from 0.4 to 0.5. The calibration error was evaluated using the relationship suggested by Bruun, 1995. This relationship is based on the standard deviation. The magnitude of the calibration errors of the current work was about 0.65-0.75%. Bruun suggested that an error of 0.2% is achievable with a carefully adjusted set up. These conditions were unavaliable in the current work and the quoted errors were considered good for the current purpose. The hot wire anemometer used in the experiments of the current work was built in the laboratory and was sucessfuly tested with a DANTEC system. These test were made in the LMF (*Fluid Mechanics Laboratory*) of the UFRGS with support of the prof. Dr. Sérgio V. Möller.

4. Non-pulsatile Flows

Previous to the study of turbulence in pulsatile flows, the variation of turbulence intensity with Reynolds. The results provided information for a comparison with the pulsating flows. The Reynolds number was set by using the valve in the

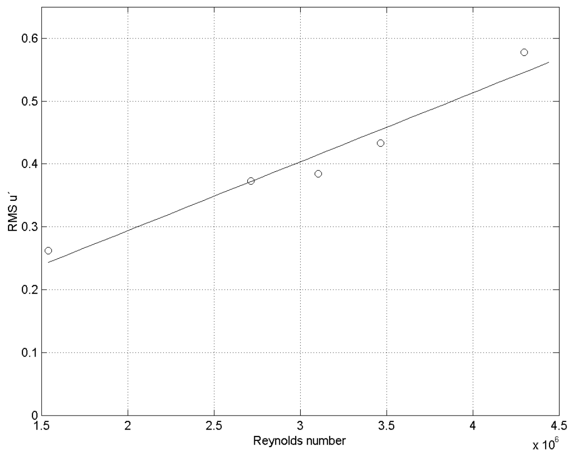

Figure 3: Turbulence intensity for non-pulsatile flows

apparatus. Frequencies below 10Hz were cutted off from the signal. The intensity of the turbulence for each Reynolds can be seen in the figure 3. The figure also gives the best linear fit to the experimental results.

As shown in figure 3, the turbulence intensity and the Reynolds number were well correlated by a linear relationship.

5. Pulsating Flows

After the non-pulsating flow analysis, we begun to study the pulsating case. The range of pulsation frequencies analysed in the current work was from 0.3 to 3Hz. This range was limited by the experimental apparatus. The data collected were digitally filtered to separate the flow parts as shown in equation 1. The cut-off frequency of the filter was chosen to be 3 times the pulsation frequency. The smoothing function used in the filter was a Hamming function. It effectively suppresses the Gibbs' effect and it can be also used on windowing procedures. The figure 4 shows $U(t)$, $\overline{U}(t)$ and $u'(t)$ for a pulsating flow with a pulsating frequency of 2Hz. A close look at the bottom frame reveals that exists a modulation of the turbulence.

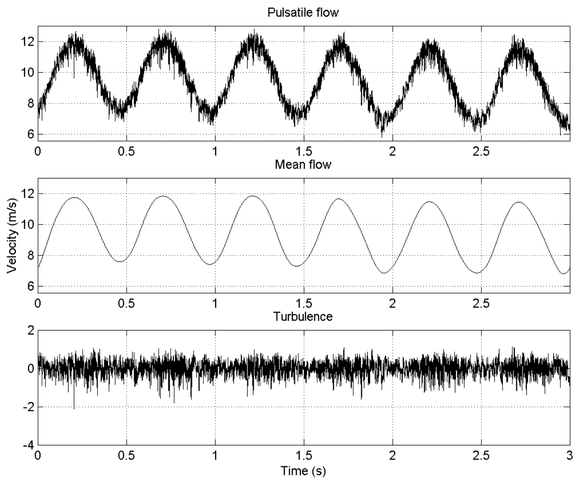

Figure 4: U(t), $\overline{U}$(t) and u'(t) for a 2Hz pulsating flow

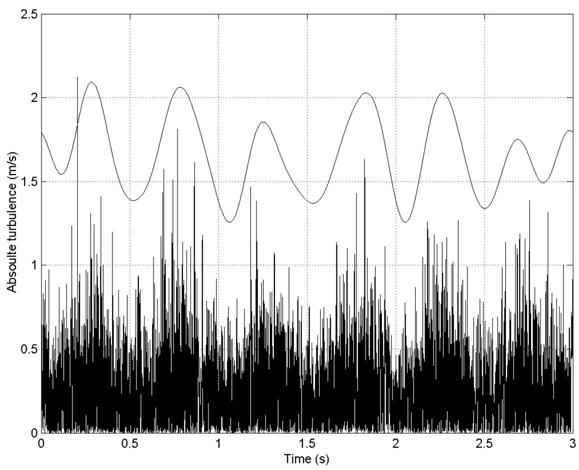

Figure 5: Turbulence intensity - 2Hz pulsation frequency

The RMS of the turbulence is shown in figure 5. A digital filtering of the RMS of the turbulence provides a measure of turbulence intensity as it varies with time. This enable a better visualization of the turbulence modulation. The cut-off frequency of the filter was 1.5 times above the pulsation frequency. The filtered signal is also shown in figure 5. It is multiplied by 3 in order to appear more clearly.

The same methodology was used for the flows with other pulsating frequencies. By the analysis of the results showed in figures 6, 7 and 8 we can observe that the turbulence intensity modulation is delayed in comparison with the base flow.

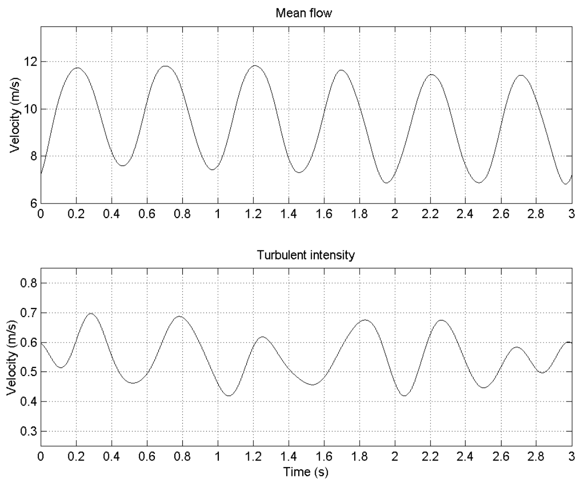

Figure 6: Mean flow and turbulence intensity -2Hz pulsation frequency

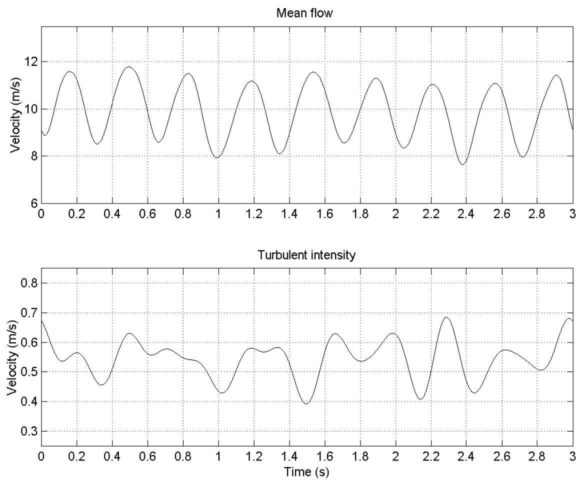

Figure 7: Mean flow and turbulence intensity -3Hz pulsation frequency

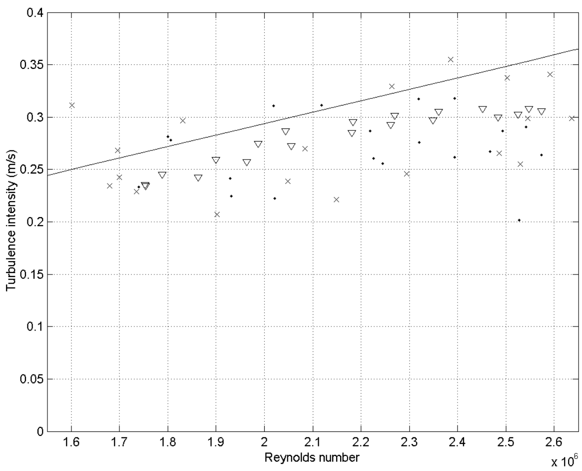

Figure 8: turbulence intensity: – non-pulsatile flow, ∇ 0.33Hz, × 2Hz and • 3Hz pulsating flows

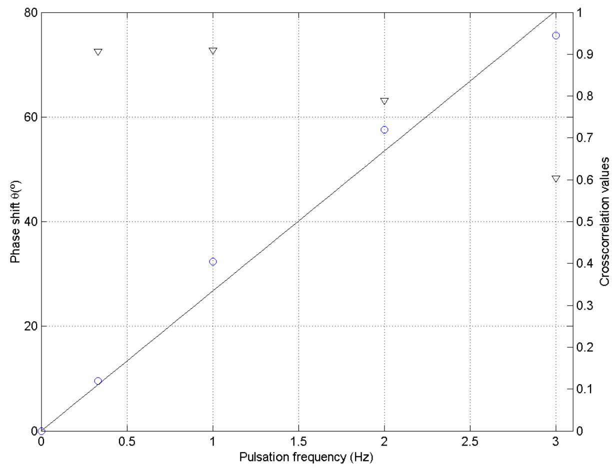

Figure 9: Phase shift between mean flow and turbulence intensity – ○ ; Cross correlation coeficient value – ∇

The amplitude of the turbulence intensity against the instant Reynolds number are shown in figure 8. The solid line is the best linear fit obtained for the non-pulsatile flows analysis which was shown in figure 3. The turbulence intensity amplitudes of non-pulsatile and the pulsatile flow of lower frequency are in reazonable agreement. This was expected because the 0.33Hz pulsating flow is a quasy steady flow. The amplitude difference can be attributed to experimental uncertainty. One might think that the previous filtering of the pulsating signal could be responsible for the reduction of turbulence intensity of these flows. However, it is not considered to be the case here because the same filtering procedure was adopted in the non-pulsating analysis. The figure also shows that the Reynolds number and the turbulence intensities are almost in phase for the low pulsation frequency of 0.3Hz. This is confirmed by tha fact that the data collected at this pulsation frequency seems to follow the linear pattern observed for the non-pulsatile case, fig. 3. This behavior cannot be seen for the other frequencies, 2 and 3Hz.

Cross correlation techniques described in Bendat and Piersol, 1971 were used to quantify the phase shift between the mean flow and the turbulence intensity. The cross correlation coefficient reaches its maximum when the two compared signals are in phase, and reaches a maximum negative value when the signals are in opposite phase that is delayed by 180^o. A zero value for a cross correlation coefficient mean that the signals are non-correlated. The time shift between the mean flow and the turbulence intensity needed to cross correlation coeficient reach this maximum value was evaluated for the range of pulsating frequencies studied. The figure 9 shows the variation of the phase shift with the pulsation frequency.

The figure also shows that the cross correlation coeficient value decreases if the pulsation frequecy is increased.

The analysis of the behavior of the turbulence spectrum along the pulsation cycle was done using time-frequency techniques. The results of the time frequency analysis are shown in the figures 10, 11 and 12. The values of the contours levels are shown close to the time axis in middle of these figures. By the time-frequency analysis it is possible to see that the turbulence spectrum changes during the pulsation cycle. However, it is more difficult to correlate the spectrum peaks with with the mean flow peaks or turbulence intensity peaks.

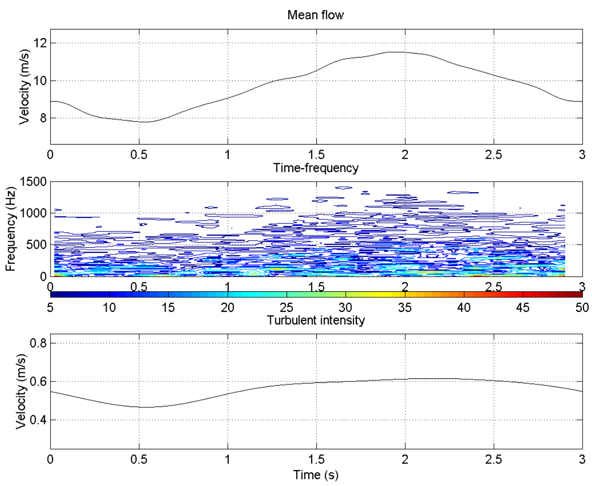

Figure 10: Time frequency analysis -.33Hz pulsating flow

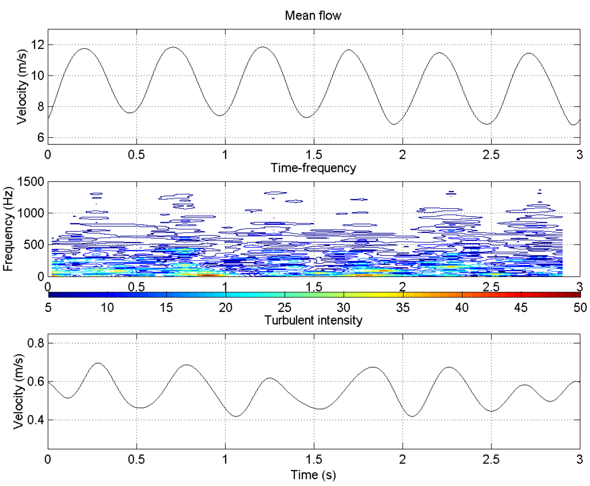

Figure 11: Time frequency analysis - 2Hz pulsating flow

6. Concluding remarks

The methodology used for the treatment of pulsating flow data seemed to work. The phase shift between turbulence intensities and the mean flow becomes higher when the pulsation frequency is increased. It was clearly shown in the figures 6, 7, 8 and 9. The figure 9 shows also that the correlation coefficient becomes lower when the pulsation frequency is increased, in that it suggests that the turbulence intensity oscillation became non-periodic at high frequencies. The results shown in this work differs of Ohmi and Iguchi, 1985. In their work about oscillating flows they suggested that the turbulence intensity peaks had occurred at instant of maximum reduction of the acceleration. The present work shows, for pulsating flows, that this point is dependent of the pulsation frequency.

The figures 10 and 11 show that the higher frequencies become more evident close to the turbulence intensity peaks. The existence of phase shift also seems to occur in the spectrum as observed for turbulence intensities. However, for the frequency of 3Hz there is no sufficient evidence to accept this affirmation. The spectrum energy for 3Hz case showed in figure 12 do not follow both the base flow and the turbulence intensity.

The present work suggests that a more detailed work can be useful for pulsatile flows studies. The analysis of the present work was limited by the experimental arrangement. An experimental arrangement with a eletronically controlled valve can be a simple way to expand the range of the experiment.

7. Acknowledgements

The first and the second authors would like to acknowledge the financial support received from FAPEMIG at the period that we developed this work and the actual financial support received from FAPESP.

The experiments were performed in the fluid mechanics laboratory of the PUC-MG. The authors would also like to acknowledge that university.

8. References

Bendat, J. S. and Piersol, A. G., 1971, “Random data - analysis and measurement procedures”, Wiley Interscience, 1^{th} edition.

Bruun, H. H., 1995, “Hot wire anemometry - principles and signal analysis”, Oxford University Press.

Catania, A. E. and Mitica, A., 1989, Extraction techniques and analysis of turbulence quantities from in cylinder velocity data, “ASME Journal of Engineering for Gas Turbines and Power”, Vol. **111**, pp. 466–478.

Catania, A. E. and Mitica, A., 1992, Time-frequency spectral structure of turbulence in an automotive engine, “SAE paper”, , No. 920153.

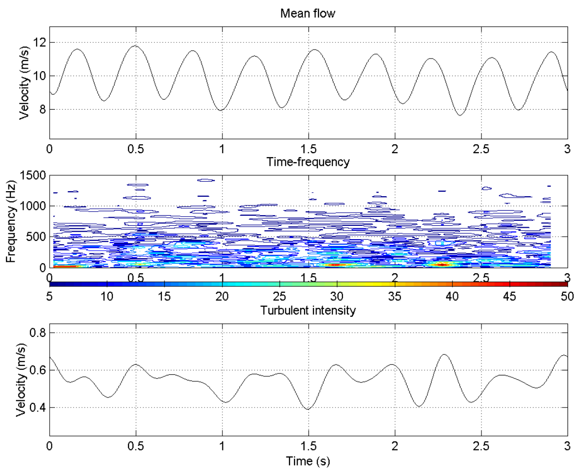

Figure 12: Time frequency analysis - 3Hz pulsating flow

Fishler, L. S. and Brodkey, R. S., 1991, Transition, turbulence and oscillating flow in pipe, “Experiments in Fluids”, Vol. **11**, pp. 388–398.

Möller, S. V., 2000, Experimentação em turbulência, “Proceedings of 2^{nd} Escola de transição e turbulência -ETT2000”, Uberlândia - MG.

Ohmi, M. and Iguchi, M., 1985, Experimental study of turbulence in a pulsatile pipe flow, “JSME paper”, , No. **264–13**.

Perry, A. E., 1982, “Hot wire anemometry”, Oxford University Press.

Schlichting, H., 1979, “Boundary layer theory”, McGraw Hill, 7^{th} edition.